

O isotope effects and vibration-rotation lines of interstitial oxygen in germanium

B. Pajot

GPS, UMR 7588, Université Denis Diderot, 2 place Jussieu, 75251 Paris Cedex 05, France

P. Clauws

Ghent University, Department of Solid State Sciences, Krijgslaan 281-S1, B-9000 Gent, Belgium

J. L. Lindström

Department of Physics, Solid State Physics, University of Lund, Lund S-22100, Sweden

E. Artacho

Departamento de Física de la Materia Condensada and Instituto Nicolas, Cabrera, C-III, Universidad Autónoma de Madrid, 28049 Madrid, Spain

(Received 29 May 2000)

The infrared absorption of interstitial ^{17}O and ^{18}O has been measured at high resolution in natural germanium in a multireflection geometry. The asymmetric mode of ^{18}O is observed to be broadened by interaction with the phonon background while that of ^{17}O is unaffected. The broadening is confirmed by results on an ^{18}O -enriched sample. All the O and Ge isotope shifts can be fitted or predicted rather accurately by a two-parameter semiempirical model using values determined by Pajot and Clauws in 1988. In the multireflection geometry, new lines of low intensity are also observed and they are ascribed to transitions with change of the rotational state of ^{16}O between the ground and excited vibrational states. Energies of the two-dimensional ^{16}O rotator are derived from these measurements, with a Ge isotope effect much smaller than the one deduced from phonon spectroscopy.

I. INTRODUCTION

When present in germanium crystals, isolated oxygen is usually located interstitially (O_i), bonded to two nearest-neighbor (NN) Ge atoms.¹ The O atom is pushed off center and the Ge-O-Ge apex angle has been estimated to be near 140° .² O_i and the two NN Ge atoms can vibrate as a quasi-isolated Ge_2O molecule with an asymmetric mode near 862 cm^{-1} at liquid helium temperature (LHeT). This mode is often noted ν_3 , by analogy with a free molecule with C_{2v} symmetry. A symmetric mode of Ge_2O at 407 cm^{-1} has also been observed indirectly from its combination mode with ν_3 , near 1270 cm^{-1} (LHeT). This symmetric mode is labeled ν_1 , accordingly. In addition to the ν_3 and ν_1 modes, theory also predicts the existence of a third mode at 213 cm^{-1} . This latter mode corresponds, like ν_1 , to a radial motion of the O atom, but while in ν_1 , the two Ge atoms move in phase with respect to the O atom, they move out of phase in this ν_2 mode.³ The nonlinear structure of the Ge-O-Ge bridge allows some kind of rotation of the O atom about the Ge-Ge axis, restricted in a plane perpendicular to the Ge-Ge axis. The energy E_0^l of this two-dimensional rotator is quantized as $Bl^2 - Dl^4$, where B is the rotational constant, D the centrifugal distortion coefficient, and l is 0 or an integer. In a classical two-dimensional (2D) vibration-rotation coupling scheme, the pseudorotation of O should couple with mode ν_2 , whose frequency comes close to the value of ω derived from the centrifugal distortion coefficient $D = 4B^3/\hbar^2\omega^3$. The eigenfunctions of the 2D rotator are $(1/\sqrt{2\pi})\exp il\phi$ with $l=0, \pm 1, \pm 2, \pm 3$, etc., but the pseu-

dorotation is weakly perturbed by the six Ge atoms second-nearest neighbors of O. This results in a small perturbing term in $\cos 6\phi$ in the potential hindering free rotation of the O atom, that splits the $\pm 3n$ rotational levels. In silicon, no splitting is detectable,⁴ but in germanium, a splitting of the ± 3 rotational levels has been detected by phonon spectroscopy.⁵ The eigenstates of the split levels are linear combinations of the -3 and $+3$ states so that they cannot be strictly labeled as pure states. For convenience, we keep however this labeling.

The pseudorotation of the O atom combines with the ν_3 mode in a coupling scheme different from the one for the free diatomic molecule. In silicon, the electric dipole of the ν_3 mode (or A_{2u} mode, when considering a $\text{Si}_3\equiv\text{Si-O-Si}\equiv\text{Si}_3$ group with D_{3d} symmetry) is essentially parallel to the Si-Si axis and thus independent of the angle of rotation ϕ .⁶ The selection rule for the rotational transitions in this particular vibration-rotation scheme is therefore $\Delta l=0$ and the observed structure is attributed to transitions where the rotational quantum number l is the same in the ground and excited vibrational states ($|0,l\rangle \rightarrow |1,l\rangle$ transitions). The same attribution has also been made in germanium: near LHeT, besides the ground state, three rotational states are populated significantly, so that four vibration-rotation lines with $\Delta l=0$, noted I, II, III, and IV, are observed.⁷ These four lines correspond to $l=0, \pm 1, \pm 2$, and -3 , respectively, and their energies decrease in this order. High-resolution spectra of $\nu_3(^{16}\text{O})$ have shown that the relatively closely spaced lines of this structure (lines I and II are separated by about 0.07 cm^{-1}) can be resolved at LHeT as the full widths at half-maximum (FWHM) are about 0.04 cm^{-1} .^{2,7,8} Line IV

is practically impossible to detect in natural germanium (${}^n\text{Ge}$) because it is very weak and obliterated by other transitions except for ${}^{76}\text{Ge}_2\text{O}$; it has been reported for the first time in quasimonoisotopic (qmi) ${}^{74}\text{Ge}$.⁷ Vibration-rotation transitions associated with ν_3 involving a change in the values of l between the ground and excited vibrational states have not been reported for O_i .

About 25 lines can be resolved in $\nu_3({}^{16}\text{O})$ when observed near LHeT. This apparent complexity is mainly due to the existence of five Ge isotopes (${}^{70}\text{Ge}$, ${}^{72}\text{Ge}$, ${}^{73}\text{Ge}$, ${}^{74}\text{Ge}$, and ${}^{76}\text{Ge}$) with abundances within the same order of magnitude. This leads to 15 different Ge_2O combinations, each with four lines. Some of these combinations, however, have the same average Ge mass, taken as the mean value of the masses of the two Ge atoms bridged to the O atom (e.g., ${}^{72}\text{Ge}_2\text{O}$ and ${}^{70}\text{Ge}{}^{74}\text{Ge}$); the corresponding transitions are thus very close to each other and difficult to resolve individually.³ For some purposes, the combinations can be defined by this Ge average mass M . For ${}^{16}\text{O}$, the average separation between corresponding lines of combinations with M and $M \pm 1$ is 0.5 cm^{-1} (see the Appendix). The spacings and the relative intensities of lines I, II, III, and IV are also such that near coincidences occur between different lines of nearby combinations. All this explains why only 25 individual lines are resolved.

The rotation of ${}^{16}\text{O}_i$ has been directly observed and measured by phonon spectroscopy below 1 K and transitions between $|0,l\rangle$ and $|0,l'\rangle$ states have been detected in ${}^n\text{Ge}$ between 1.3 and 4.8 meV (about 10.5 and 38 cm^{-1}) without strict selection rules.⁵ The energies of the first rotational levels in the vibrational ground state have been deduced from these measurements and the values calculated using a hindered rotator model are in good agreement with the experimental ones.³ The combination with the vibration-rotation data in the midinfrared allows to determine the spacings of the rotational levels in the excited vibrational state. They are slightly smaller than in the ground state.

The vibration-rotation spectrum of ${}^{18}\text{O}$ has been previously observed in germanium at low resolution or with a poor signal/noise ratio,^{8,9} and there is no information on ${}^{17}\text{O}_i$. It could be interesting however to compare the situation in germanium with that in silicon, where a resonance effect broadens the $\nu_3({}^{17}\text{O})$ structure.¹⁰

We report here results obtained from good-quality $\nu_3({}^{17}\text{O})$ and $\nu_3({}^{18}\text{O})$ spectra in germanium with ${}^{17}\text{O}$ and ${}^{18}\text{O}$ natural abundances. The ${}^{18}\text{O}$ spectra are compared with those in a sample enriched with ${}^{18}\text{O}$. In the present paper, weak sidebands of the $\nu_3({}^{16}\text{O})$ structure have also been observed and their origin is discussed.

II. EXPERIMENTAL RESULTS

In order to detect $\nu_3({}^{17}\text{O})$ and $\nu_3({}^{18}\text{O})$, a standard (S) Ge:O sample with a high O concentration was chosen [$\sim 2.5 \times 10^{17} \text{ at/cm}^3$ using a calibration factor¹¹ of $5 \times 10^{16} \text{ at/cm}^{-2}$ for the room temperature absorption of the $\nu_3({}^{16}\text{O})$ mode at 855.7 cm^{-1}] and a trapezoidal geometry adopted. With this geometry, the infrared (IR) beam enters normal to one side of the sample, cut at 45° , makes several total reflections, and exits by the other side, parallel to the first. Considering the dimensions of the sample, an effective

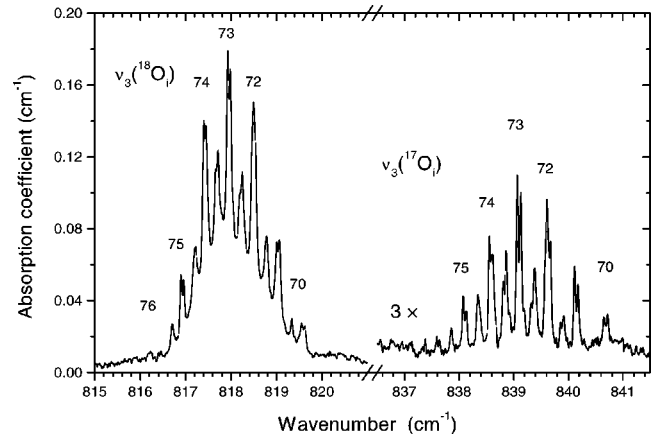


FIG. 1. Compound spectrum of $\nu_3({}^{18}\text{O})$ and $\nu_3({}^{17}\text{O})$ at 6 K in sample S with $[\text{O}_i]$ near $2.5 \times 10^{17} \text{ atoms/cm}^3$ ($[\text{O}_i]$ are about 5 and $1 \times 10^{14} \text{ atoms/cm}^3$, respectively). Some of the average or true Ge masses are indicated above the pair of lines I and II. Note the background superimposed to $\nu_3({}^{18}\text{O})$, due to an O-related defect mode. The apodized resolution is 0.02 cm^{-1} .

path length of the optical beam $\sim 22 \text{ mm}$ is obtained. This sample was fitted in a specially designed sample holder for a continuous flow Oxford Instruments optical cryostat, and cooled in He gas at approximately 6 K. Another sample was ${}^{18}\text{O}$ -enriched (OE) and used in the normal transmission geometry. With the same calibration factor as before, the concentrations of ${}^{16}\text{O}_i$ and ${}^{18}\text{O}_i$ in this sample are about 5 and $33 \times 10^{15} \text{ at/cm}^3$, respectively. The IR measurements were performed in the $230\text{--}1000 \text{ cm}^{-1}$ spectral range with BOMEM DA3+ and DA8 Fourier-transform spectrometers, using either a MCT detector with a cutoff at 700 cm^{-1} or a silicon bolometer.

The S sample had been annealed near 900°C and quenched to destroy the thermal donors (TD's) present in the as-grown material.¹² This is necessary to reduce to a minimum the continuum electronic absorption because of the relatively long optical path through the sample. At room temperature, in the S sample, besides $\nu_3({}^{16}\text{O})$, a weak band with a FWHM of 4.9 cm^{-1} is also measured at 813.6 cm^{-1} . This band is distinct from $\nu_3({}^{18}\text{O})$, observed at 811.8 cm^{-1} in the OE sample, and its origin is discussed below.

The high-resolution spectrum of the S sample at LHeT shows the ν_3 mode of the three O isotopes (the natural proportions of ${}^{16}\text{O}$, ${}^{17}\text{O}$, and ${}^{18}\text{O}$ are approximately 100, 0.04, and 0.2, respectively) and two weak and rather broad bands at 780 and 801 cm^{-1} . The composite spectrum of Fig. 1 shows $\nu_3({}^{17}\text{O})$ and $\nu_3({}^{18}\text{O})$ near 6 K. It looks as if a broadband was superimposed to the $\nu_3({}^{18}\text{O})$ structure while nothing conspicuous is seen for $\nu_3({}^{17}\text{O})$. Three bands at 780, 801, and 819 cm^{-1} have indeed been reported in O-containing germanium irradiated at liquid nitrogen temperature with high-energy electrons, after annealing at 200°C .⁹ The same bands also appear as weak features in O-doped germanium after a dispersion quench from elevated temperature and this is the reason for their observation in sample S. As the 819 and 780 cm^{-1} bands disappear again during the initial stage of a 350°C annealing sequence, it has been suggested in this context that the center giving the

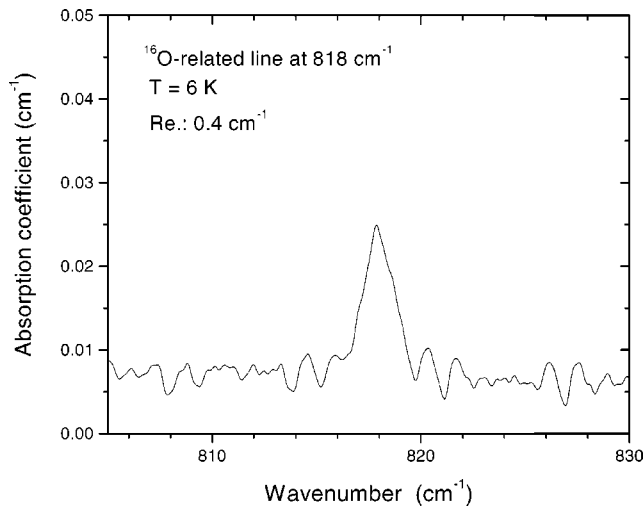


FIG. 2. Difference spectrum of S sample before and after annealing for 5 min at 350 °C showing the ^{16}O -related vibrational mode responsible for the background of $\nu_3(^{18}\text{O})$. The intensity of this mode corresponds to the fraction (about 40%) of corresponding centers destroyed by the annealing at 350 °C (see the text).

819 cm^{-1} band is the O_2 dimer.¹³ The S sample was thus annealed under flowing argon gas for 5 min at 350 °C. This produced a reduction of the intensity of the 780 cm^{-1} band and of the background of $\nu_3(^{18}\text{O})$ while a small increase of the band at 801 cm^{-1} was observed. The reduction of the background can be appreciated quantitatively by subtracting the $\nu_3(^{18}\text{O})$ spectrum after this second annealing from the initial spectrum: the result is a weak line at 817.8 cm^{-1} with a FWHM of 1.8 cm^{-1} , clearly seen in Fig. 2. This line is the ‘‘819 cm^{-1} ’’ band, superimposed to $\nu_3(^{18}\text{O})$ in the S sample. This line is the one observed at 813.6 cm^{-1} at room temperature. In Fig. 2, its intensity corresponds to the fraction (estimated to 40%) of the centers produced by the quenching from 900 °C that have been dissociated by the annealing at 350 °C. No other annealing of the sample was performed in order to avoid further production of TD’s. Another particularity of $\nu_3(^{18}\text{O})$ is that the individual lines are broader than those for ^{16}O and ^{17}O . In order to better appreciate the effect, a full subtraction of the broad band from the spectrum of sample S was performed. The corrected $\nu_3(^{18}\text{O})$ profile is then very comparable to the one obtained with the OE sample. The $\nu_3(^{18}\text{O})$ absorption in this latter sample is shown in Fig. 3, with nearly the same background as the one observed for the other O isotopes. The increase of the widths from $M = 76$ to 70 in $\nu_3(^{18}\text{O})$ is attested from the decrease of the resolution of components I and II for decreasing values of M . For masses 72 and 74, the comparison is difficult because they can be obtained with different combinations of Ge isotopes that give slightly frequencies, preventing normal resolution of components I and II. A possible cause of the increase of the $^{18}\text{O}_i$ linewidths with respect to those of $^{17}\text{O}_i$ and $^{16}\text{O}_i$ is a resonant interaction with the three-phonon background of germanium. Only in qmi ^{70}Ge and in ^{76}Ge samples could the situation differ because of the shift of the phonon spectrum in the qmi samples compared to ^nGe ($n = 72.6$ amu). This should change the strength of the interaction between the local mode and the phonon density-of-

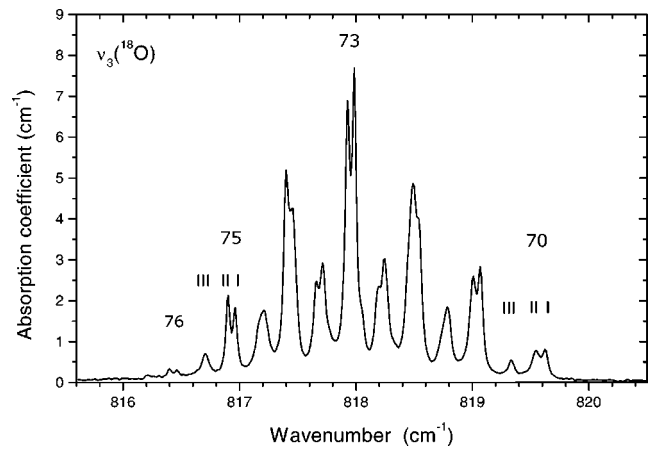


FIG. 3. Absorption at 6 K of $\nu_3(^{18}\text{O})$ in the Ge sample with $[^{18}\text{O}_i] = 3.3 \times 10^{16}$ at/cm^3 . Some of the Ge masses are indicated above the pair of lines I and II. Note the change on the resolution of components I and II for $M = 70$ and 75 and the observation of the components for $M = 76$. The apodized resolution is 0.02 cm^{-1} .

states and a small shift of the $\nu_3(^{18}\text{O})$ lines could eventually be observed, similar to the effects observed with $\nu_3(^{16}\text{O})$.¹⁴ The broadening of the components of $\nu_3(^{18}\text{O})$ also shows up on the maximum absorption of this band: if the linewidths were the same for $\nu_3(^{18}\text{O})$ and $\nu_3(^{17}\text{O})$, the ratio of the maximum absorptions $I_{\text{max}}(^{18}\text{O})/I_{\text{max}}(^{17}\text{O})$ in sample S should match the ratio of the natural isotopic abundances. Now, after subtraction of the contribution of the 819 cm^{-1} line to the intensity of $\nu_3(^{18}\text{O})$, the ratio $I_{\text{max}}(^{18}\text{O})/I_{\text{max}}(^{17}\text{O})$ is ~ 3 while a value of 5 is expected. The frequencies of components of $\nu_3(^{18}\text{O})$ and $\nu_3(^{17}\text{O})$ that can be identified with a minimum of interferences with other lines are listed in Table I. The values for $\nu_3(^{18}\text{O})$ are in good agreement with those given in Ref. 8. As mentioned before, the widths of the

TABLE I. Frequencies (cm^{-1}) at 6 K of lines I, II, and III of $\nu_3(^{18}\text{O})$ and $\nu_3(^{17}\text{O})$ in natural germanium for some values of the average Ge mass M . Missing values are due to strong interferences or to components too weak for detection.

O isotope	M (amu)	Line I	Line II	Line III
^{18}O	70	819.62	819.55	819.33
^{17}O	70	840.72	840.65	
^{18}O	71	819.07	819.01	818.79
^{17}O	71	840.18	840.11	839.90
^{18}O	72	818.54	818.48	
^{17}O	72	839.68		
^{18}O	72.5		818.19	
^{17}O	72.5		839.32	
^{18}O	73	817.98	817.93	
^{17}O	73	839.13	839.07	838.86
^{18}O	73.5		817.67	
^{18}O	74	817.45	817.40	
^{17}O	74	838.62	838.55	
^{18}O	75	816.96	816.90	816.71
^{17}O	75	838.14	838.07	837.86
^{18}O	76	816.46	816.40	816.2

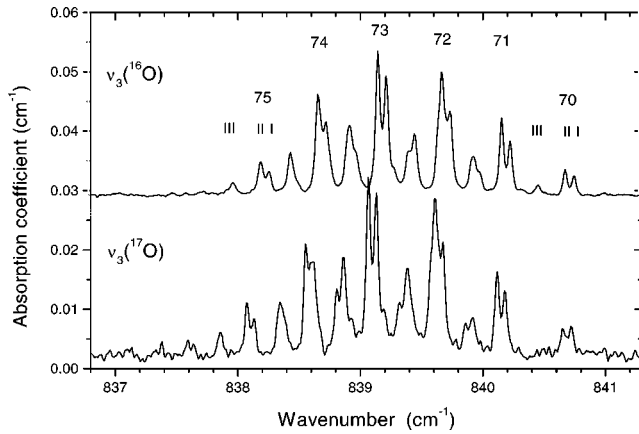


FIG. 4. Comparison of $\nu_3(^{17}\text{O})$ in sample S with $\nu_3(^{16}\text{O})$ at 6 K in a ^{76}Ge sample with $[\text{O}_i] = 8 \times 10^{15}$ atoms/cm³. Some of the Ge masses are indicated above the pair of lines I and II. For $M = 70$ and 75, lines I, II, and III are indicated. Differences in the profiles are due to the slightly smaller spacings between lines I, II, and III for ^{17}O . The abscissa scale and the resolution (0.02 cm^{-1}) are the same for both spectra as for Fig. 3. The ^{16}O spectrum is displayed between 860 and 864.5 cm^{-1} .

components of the ^{17}O band are comparable to those of ^{16}O (Fig. 4). There is a slight increase of the Ge isotope shift when going from ^{16}O to ^{17}O , visible in Fig. 4. Inversely, the separations between components I, II, and III for the same value of the Ge mass, slightly decrease from ^{16}O to ^{18}O . These changes in the spacings produce in turn small changes in the overall profiles of the bands. In all the series of spectra we have obtained, it was very difficult or impossible to observe component III ($^{70}\text{Ge}_2^{17}\text{O}$), whatever the detector used. Inversely, lines which could have been attributed to components I and II of $\nu_3(^{76}\text{Ge}_2^{17}\text{O})$ have been observed in the two spectra with the best signal-to-noise ratio, despite the very small intensity expected.

The absorption of the S sample in the normal transmission geometry has also been measured in the 400 cm^{-1} range at LHeT to try to detect the ν_1 mode (in this range, the two-phonon absorption of the Ge lattice forbids the use of a multireflection geometry). However, when careful subtraction of the phonon background is performed, no absorption is detected. This is likely to be due to the small dipole moment associated with the mode, combined with a predicted half-width near 10 cm^{-1} . On the other hand, the $\nu_1 + \nu_3$ combination mode of $^{18}\text{O}_i$ could be detected in the OE sample at 1215.8 cm^{-1} . The exact position for $^{16}\text{O}_i$ is 1269.4 cm^{-1} , hence a ^{16}O - ^{18}O isotope shift of 53.6 cm^{-1} for this combination. From a comparison with the averaged ^{16}O - ^{18}O isotope shift of ν_3 (see legend of Table III), the corresponding shift for ν_1 is found to be only 9.3 cm^{-1} , indicating a smaller amplitude of the O atom in this particular vibration as compared to the motion of the Ge atoms.³ The same O isotope shift is only 1.2 cm^{-1} for the ν_1 mode of O_i in silicon¹⁰ and such a small value is due to the nearly linear structure of the Si-O-Si bridge.

In the S sample, $\nu_3(^{16}\text{O})$ saturates because of the optical path length, but a series of weak and relatively sharp features are observed on both sides of this band (Fig. 5). The most intense series of lines is shown in Fig. 6 on an expanded

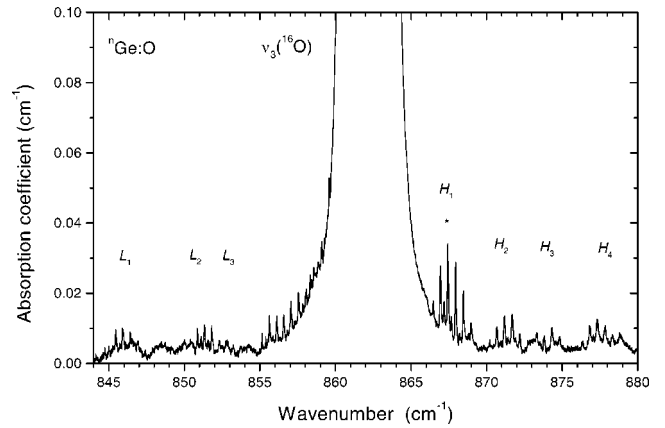


FIG. 5. Sidebands of $\nu_3(^{16}\text{O})$ at 6 K showing different series of isotopic lines. The intensity of the starred line ($M = 73$) is about 4×10^{-4} times the peak absorption for this mass for $\nu_3(^{16}\text{O})$.

scale: it displays the same Ge isotope effect as the ^{16}O central band, but with only one transition for each Ge combination instead of four in the central band. These Ge isotopic series are clearly related to the central band and those on the high-energy side look more intense than those on the low-energy side. In a spectrum obtained at 15 K, a small relative decrease of the intensity of the high-energy features compared to the low-energy ones was observed. It is difficult to obtain significant data above 15 K because of the broadening of the lines. We none the less interpret the high-energy side series as transitions where the value of the rotational quantum number l of ^{16}O is lower in the vibrational ground state than in the excited state and the inverse for the low-energy series. These high-energy series are labeled H_1 , H_2 , H_3 , and H_4 in order of increasing energies. Two series of lines comparable to the preceding ones are observed on the low-energy side of $\nu_3(^{16}\text{O})$ and two lines pertaining to a third series are also detected. These latter series are labeled L_1 , L_2 , and L_3 . From their relative intensities, it has been possible to attribute the lines within a series to definite values of the Ge mass, averaged or not, and the result is given in Table II. About 20 more or less equally spaced lines, which can contain Ge isotopic series, are also found between 855

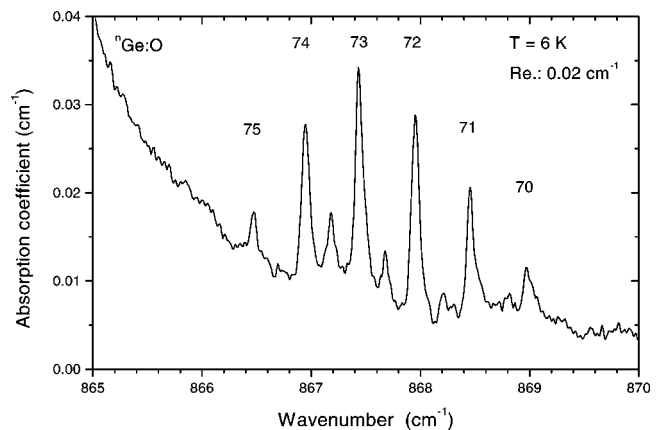


FIG. 6. Closeup of the H_1 series ascribed to the $|0,0\rangle \rightarrow |1,\pm 2\rangle$ vibration-rotation transition of $^{16}\text{O}_i$ showing Ge isotopes attribution. The FWHM of the components is about 0.08 cm^{-1} .

TABLE II. Frequencies (cm^{-1}) at 6 K of lines of H and L sidebands series of $\nu_3(^{16}\text{O})$ band ascribed to definite values of M . The predicted RI, deduced from natural Ge isotopic abundances, are normalized to that for $M=71$.

H_1	H_2	H_3	H_4	L_1	L_2	L_3	M (amu)	RI
							76	0.05
866.47	870.21		876.36	845.00			75	0.51
866.7							74.5	0.11
866.95	870.69	873.32	876.84	845.56	850.86	852.3	74	1.57
867.18	870.93				851.10		73.5	0.51
867.43	871.17	873.81	877.32	845.94	851.33	852.8	73	2.12
867.67	871.41				851.6		72.5	0.38
867.95	871.69	874.32	877.84	846.41	851.81		72	2.01
868.21							71.5	0.29
868.46	872.19	874.84	878.33	846.92	852.3		71	1.00
868.97				847.43			70	0.38

and 860 cm^{-1} , at the base of $\nu_3(^{16}\text{O})$ and attributions for some of them are discussed later. The lines of the H and L series are typically 10^{-4} – 3×10^{-4} times less intense than the corresponding lines of the $\nu_3(^{16}\text{O})$ band.

III. DISCUSSION

A. The $\nu_3(^{17}\text{O})$ and $\nu_3(^{18}\text{O})$ bands

First, from the comparison of the O_i spectra in silicon and in germanium, it seems that the broadening observed for $\nu_3(^{17}\text{O})$ in silicon is due to a resonance effect and not to the nature of the O isotope. In germanium, $\nu_3(^{18}\text{O})$ is at the same frequency as a local mode related to ^{16}O , but it is difficult to understand how the two modes can interact as they are both localized. The intensity of the low-temperature three-phonon background is nearly the same for the three O isotopes, but we assume that $\nu_3(^{18}\text{O})$ is broadened by a resonance with a three-phonon combination at a frequency sufficiently close to the high-energy side of this band. The Ge isotopes shifts of the components of the $\nu_3(^{16}\text{O})$ band have first been modeled in a quasifree molecule approximation, neglecting the coupling with rotation. For a nonlinear symmetric triatomic Ge-O-Ge molecule with an apex angle 2α , a value of the ratio $\nu_3(^i\text{Ge}_2\text{O})/\nu_3(\text{Ge}_2\text{O})$, where the index i denotes any isotopic substitution, can be determined within the central forces framework:

$$\frac{\nu_3(^i\text{Ge}_2\text{O})}{\nu_3(\text{Ge}_2\text{O})} = \sqrt{\frac{M_{\text{Ge}}M_{\text{O}}(M_{i\text{O}} + 2M_{i\text{Ge}}\sin^2\alpha)}{M_{i\text{Ge}}M_{i\text{O}}(M_{\text{O}} + 2M_{\text{Ge}}\sin^2\alpha)}}, \quad (1)$$

where M_X is the mass of atom X .¹⁵ To take into account the binding of the quasimolecule with the crystal, an interaction mass m' was added empirically to the mass of the Ge atom. The value of this interaction mass and of the apex angle 2α had to be determined self-consistently by a best-fit procedure with a selected experimental shift.² The first determination yielded $m' = 11.65 \text{ amu}$ and $2\alpha = 140^\circ$.² Another set of values (23.1 amu and 111°) has been obtained from slightly different experimental values using a more restricted fitting range.⁸ The former set (11.65 amu and 140°) has been tested by computing all the frequencies of components II for the three O isotopes and for different values of the Ge mass for

^{70}Ge . With only one experimental frequency [component II($^{70}\text{Ge}_2^{16}\text{O}$) in ^{70}Ge at 863.853 cm^{-1}] as $\nu_3(\text{Ge}_2\text{O})$ in expression (1), the maximum deviation with the experimental values using this set is 0.05 cm^{-1} . With the set (23.1 amu , 111°), deviations as large as 0.6 cm^{-1} are found with the same procedure. For this reason, we think the set of Ref. 2 is physically more significant.

Within this model, a value of 0.6 \AA is obtained for the distance between the O atom and the Ge-Ge axis (a Ge-O bond length of 1.74 \AA is assumed). This value is very close to the one derived from an *ab initio* calculation using a cluster-Hartree-Fock approximation, intended to determine the radial potential limiting the O motion.³ The vibration modes of this system can be obtained in the cluster-Bethe-lattice approximation.¹⁶ Isotope effects can thus be calculated by making the suitable isotopic changes. Significant Ge and O isotope shifts are summarized in Table III. This table shows that the calculations predict accurately the O isotope shift, determined for a Ge mass of 73 amu , while the Ge shifts, determined by replacing all the atoms of the cluster by the same Ge isotope, are overestimated.

The rotation of the O atom shows up indirectly in the splittings between components I, II, III, and IV. These splittings represent the differences between the same rotational energy levels in the vibrational ground and excited states. For ^{16}O , the splittings are 0.07 , 0.30 , and 0.78 cm^{-1} for I–II, I–III, and I–IV, respectively. For ^{18}O , the I–II and I–III spacings measured for $M=75$, where the resonant broadening effect is thought to be weak, decrease to 0.06 and 0.28 cm^{-1} (uncertainty: $\pm 0.01 \text{ cm}^{-1}$). Values of the first rotational energy levels of ^{16}O deduced from phonon spectroscopy are listed in Table IV. Phonon spectroscopy has also been performed on a ^{70}Ge sample implanted with ^{18}O . The rotational energies for this isotope are smaller by a factor 0.935 than the ones for ^{16}O , while a ratio $0.889 = 16/18$ is expected.¹⁷ This larger value has been explained by assuming that the Ge atoms bonded to the O atom accompany its rotation.³ This seems to be confirmed by the observation of Ge isotope shifts of the ^{16}O rotational transitions in qmi Ge samples, which are too large to be explained by only the effect of the change of the average lattice mass.¹⁷

TABLE III. Three first rows: comparison of the experimental values of the $\text{II}({}^{70}\text{Ge})\text{-II}({}^{75}\text{Ge})$ spacings (cm^{-1}) for the three O isotopes with: the values from the central-forces molecular model (Semiempirical) and from theory. Four last rows: ${}^{16}\text{O}\text{-}{}^{17}\text{O}$ and ${}^{16}\text{O}\text{-}{}^{18}\text{O}$ isotope shifts for $\text{II}({}^{70}\text{Ge})$ and $\text{II}({}^{75}\text{Ge})$. For (a), the interaction parameter mass m' is 11.65 amu and the angle 2α of the bent Ge-O-Ge group is 140° ; for (b), m' is 23.1 amu and 2α is 111° . $M=75$ amu (${}^{74}\text{GeO}{}^{76}\text{Ge}$) is chosen rather than $M=76$ amu because of its intensity. The low-resolution averaged values at LHeT of the ${}^{17}\text{O}$ and ${}^{18}\text{O}$ isotopes shifts with respect to ${}^{16}\text{O}$ are 23.3 and 44.3 cm^{-1} , respectively.

	Exper.	Semiempir. (a)	Semiempir. (b)	Theory
${}^{16}\text{O}$ (${}^{70}\text{Ge}\text{-}{}^{75}\text{Ge}$)	2.49	2.49	2.48	3.30
${}^{17}\text{O}$ (${}^{70}\text{Ge}\text{-}{}^{75}\text{Ge}$)	2.58	2.56	2.54	3.39
${}^{18}\text{O}$ (${}^{70}\text{Ge}\text{-}{}^{75}\text{Ge}$)	2.65	2.62	2.61	3.49
${}^{70}\text{Ge}$ (${}^{16}\text{O}\text{-}{}^{17}\text{O}$)	23.20	23.18	22.86	23.20
${}^{75}\text{Ge}$ (${}^{16}\text{O}\text{-}{}^{17}\text{O}$)	23.28	23.25	22.94	23.29
${}^{70}\text{Ge}$ (${}^{16}\text{O}\text{-}{}^{18}\text{O}$)	44.30	44.34	43.71	44.34
${}^{75}\text{Ge}$ (${}^{16}\text{O}\text{-}{}^{18}\text{O}$)	44.46	44.47	43.84	44.54

B. The sidebands of $\nu_3({}^{16}\text{O})$

For the interaction of the rotation of the O atom with the ν_3 mode, the selection rule $\Delta l=0$ is strictly valid for a linear configuration of the quasimolecule. The Ge-O-Ge group is clearly not linear, so that the dipole moment of the ν_3 mode has a component perpendicular to the Ge-Ge axis, which can allow vibration-rotation transitions with $\Delta l \neq 0$. In order to explain the origin of the Ge isotope series of Table II, we have determined the approximate position of the first transitions with $\Delta l = \pm 1$ and ± 2 . Using the values of Table IV and of the table in the Appendix, the first four transitions with $\Delta l = +1$ for $M=73$ amu are found to be located between 863.7 and 871.8 cm^{-1} . In any case, the $|0,0\rangle \rightarrow |1, \pm 1\rangle$ transition cannot be observed because of the intense absorption at the center of the band, but the three other ones could be. There are no lines observed near the predicted positions and the H lines extend between 867.4 and 877.3 cm^{-1} . For $\Delta l = +2$ transitions, there is a reasonable agreement between the predicted frequencies (867.5 , 871.3 , and 877.1 cm^{-1}) of the $|0,0\rangle \rightarrow |1, \pm 2\rangle$, $|0, \pm 1\rangle \rightarrow |1, -3\rangle$, and $|0, \pm 2\rangle \rightarrow |1, \pm 4\rangle$ transitions for $M=73$ amu and those of $H_1(73)$, $H_2(73)$, and $H_4(73)$ in Table II. This can provide guidelines for the attribution of the sidebands of $\nu_3({}^{16}\text{O})$. The $\Delta l = -2$ selection rule has also been tried for the L series. There again, the agreement seems reasonable: the $|0, \pm 2\rangle \rightarrow |1, 0\rangle$ transition for $M=73$ amu is predicted at 857.0 cm^{-1} and in the set of more or less equally spaced lines at the base of $\nu_3({}^{16}\text{O})$, one line is found at 857.06 cm^{-1} , that is ascribed to that transition. The $|0, -3\rangle \rightarrow |1, \pm 1\rangle$ transition is predicted at 852.8 cm^{-1} compared to 852.8 cm^{-1} for $L_3(73)$. The $|0, +3\rangle \rightarrow |1, \pm 1\rangle$ tran-

sition is predicted at 850.6 cm^{-1} , but no line is observed near this frequency. This absence could be due to the combination of a population effect with a smaller transition probability. Series L_1 is attributed to the $|0, \pm 4\rangle \rightarrow |1, \pm 2\rangle$ transition, despite the fact that the $|0, \pm 4\rangle$ state is only weakly populated at 6 K. The reason is here again the good agreement between the predicted and observed values and the fact that all the other possible combinations predict frequencies larger than the ones observed. L_2 (73) at 851.33 cm^{-1} is quite close to the value of 851.3 cm^{-1} predicted for the frequency of the $|0, -3\rangle \rightarrow |1, 0\rangle$ transition; inversely, no high-frequency line could be attributed to the $|0, 0\rangle \rightarrow |1, -3\rangle$ transition, predicted at 872.7 cm^{-1} . These results are given for $M=73$ amu, but comparable results are obtained for $M=71$, 72 , and 74 amu. They show that vibration-rotation transitions, not obeying strict selection rules, are observed in the present case. In Table V, derived from the preceding attributions, the rotational energies are expressed in terms of those of the different vibration-rotation lines observed. The only plausible attribution for the H_3 series is the $|0, \pm 1\rangle \rightarrow |1, +3\rangle$ transition. For $M=73$ amu, the predicted value is 873.5 cm^{-1} , to compare with 873.8 cm^{-1} for $H_3(73)$, a value significantly larger than expected. For the vibrational ground state, the agreement with the rotational energies obtained from phonon spectroscopy is good, and this seems to confirm the validity of our attributions. The energy of the $|0, +3\rangle$ level could however not be determined as no transition originating from this level has been identified. From the good agreement between the two methods, the energy of the $|0, +3\rangle$ level given in Table V obtained by adding to the value for $|0, -3\rangle$ the value for the

TABLE IV. Second row: experimental values (cm^{-1}) of the energies above the ground state of the first rotational levels of ${}^{16}\text{O}$ in ${}^n\text{Ge}$ derived from phonon spectroscopy (Ref. 18). The values in meV are given in parentheses. Last row: estimation of the energies of these levels in the excited vibrational state, derived from the mid-IR data. The $l = +3$ and ± 4 values in brackets are extrapolated by assuming that they are 5% smaller than in the vibrational ground state.

$l = \pm 1$	$l = \pm 2$	$l = -3$	$l = +3$	$l = \pm 4$	$l = \pm 5$
1.4 (0.17)	5.4 (0.67)	10.9 (1.35)	13.1 (1.63)	21.1 (2.62)	32.6 (4.04)
1.3	5.1	10.1	[12.5]	[20.1]	

TABLE V. Spacings of the first rotational levels of ^{16}O in ^nGe expressed as functions of combinations of the mid-IR lines observed in this paper and before. With regard to the frequencies, $L_3 = \text{I} + \text{IV} - H_2$. The numerical values are determined using the frequencies for $M = 73$. For $M = 70$ and 75 , the values of the $|0, -0\rangle - |1, \pm 4\rangle$ spacing are 21.54 and 21.47 cm^{-1} , respectively. For the $|0, 0\rangle - |0, +3\rangle$ spacing, see the text.

Spacing	IR combination	Energy (cm^{-1})
$ 0, 0\rangle - 0, \pm 1\rangle$	$\text{I} + \text{IV} - (H_2 + L_2)$	1.50
$ 0, 0\rangle - 0, \pm 2\rangle$	$H_1 - \text{III}$	5.34
$ 0, 0\rangle - 0, -3\rangle$	$\text{I} - L_2$	11.07
$ 0, 0\rangle - 0, +3\rangle$		[13.26]
$ 0, 0\rangle - 0, \pm 4\rangle$	$H_1 - L_1$	21.49
$ 1, 0\rangle - 1, \pm 1\rangle$	$\text{II} + \text{IV} - (H_2 + L_2)$	1.43
$ 1, 0\rangle - 1, \pm 2\rangle$	$H_1 - \text{I}$	5.03
$ 1, 0\rangle - 1, -3\rangle$	$\text{IV} - L_2$	10.27
$ 1, 0\rangle - 1, +3\rangle$	$L_3 + H_3 - (\text{II} + L_2)$	12.95
$ 1, 0\rangle - 1, \pm 4\rangle$	$H_1 + H_4 - (\text{I} + \text{III})$	20.26

$|0, -3\rangle - |0, +3\rangle$ spacing obtained by phonon spectroscopy for ^nGe .¹⁷ The numerical values of Table V are in line with the decrease of the rotational energies in the vibrational excited state, but we note that the $|0, -3\rangle - |0, +3\rangle$ splitting is smaller than the $|1, -3\rangle \rightarrow |1, +3\rangle$ splitting.

As already mentioned, a Ge isotope effect on the rotational energies has been measured by phonon spectroscopy using qmi Ge samples. It has been interpreted as due to an accompanying motion of the two Ge atoms NNs of the O atom during the rotation, which consequently reduces the rotational energies with increasing masses of the Ge isotopes. However, the width of the phonon resonances in ^nGe are smaller than what is expected from a superposition of the shifts due to the different Ge isotopes bound to the O atom. This could be explained by a large interaction with the lattice, which averages the Ge masses, but this seems to be contradicted by the existence of a Ge isotope shift of the ν_3 mode and the small FWHM of the lines. From the IR results, a shift of $-0.07 \pm 0.04 \text{ cm}^{-1}$ of the $|0, 0\rangle \rightarrow |0, \pm 4\rangle$ rotational energies is found between $M = 70$ amu and $M = 75$ amu. This value is smaller by nearly an order of magnitude than the corresponding shift measured by phonon spectroscopy between qmi ^{70}Ge and the mean of qmi ^{74}Ge and ^{76}Ge for the same transition.¹⁷ This can be interpreted as a reduction of the amplitude of the displacement of the two Ge atoms from the Ge-Ge axis at rest accordingly and it seems to show that the role of the average mass of the lattice in this kind of isotope shift has to be reconsidered. This result also differs from the conclusions drawn from the already mentioned ratio of the $|0, \pm 4\rangle$ rotational energies measured for ^{16}O and ^{18}O in ^nGe . This ratio was closer to unity than the value $\frac{16}{18}$ expected when considering the rotation of the O atom alone. In that case, it could be due to the nature of the ^{18}O -implanted Ge sample, where the implanted zone has a lattice parameter different from the unimplanted one and phonon resonance experiments on bulk samples enriched with ^{18}O are desirable to fix this point.

From Table V the energies of the $\Delta l = 0$ $|0, +3\rangle \rightarrow |1, +3\rangle$ and $|0, \pm 4\rangle \rightarrow |1, \pm 4\rangle$ transitions for

$M = 73$ amu are $I - 0.31 \text{ cm}^{-1}$ and $I - 1.23 \text{ cm}^{-1}$, respectively. The $|0, +3\rangle \rightarrow |1, +3\rangle$ transition is very close to line III ($I - 0.30 \text{ cm}^{-1}$) and its detection would be very difficult. For $M = 76$ amu, the $|0, \pm 4\rangle \rightarrow |1, \pm 4\rangle$ transition should be located at 859.7 cm^{-1} and no line occurs at this exact frequency. This line should be weak because of the population of the level and of transition probabilities, but we could expect to detect it. The energies of the $|0, \pm 2\rangle \rightarrow |1, \pm 1\rangle$ and of the $|0, -3\rangle \rightarrow |1, \pm 2\rangle$ transitions for $M = 73$ amu have been calculated from Table V. They are 858.51 and 856.36 cm^{-1} , respectively. If one line at 858.57 cm^{-1} could be ascribed to $|0, \pm 2\rangle \rightarrow |1, \pm 1\rangle$, the line closest to a possible $|0, -3\rangle \rightarrow |1, \pm 2\rangle$ transition is at 856.58 cm^{-1} and the attribution is unlikely. Many lines among those between 855 and 860 cm^{-1} have not been attributed and we note that some of them have a FWHM near 0.03 cm^{-1} . It has been checked that they are not due to residual gases in the interferometer. The surface of the sample has been properly cleaned, but not etched so that the possibility that some of these lines arise from an unwanted attenuated total reflection spectrum of surface contaminants cannot be excluded.

IV. CONCLUSION

Low-temperature IR measurements on a natural Ge:O sample using a multireflection geometry have allowed us to obtain high-resolution spectra of the asymmetric ν_3 mode of interstitial ^{17}O and ^{18}O . They show that the widths of the ^{17}O lines are comparable to those of ^{16}O while those of ^{18}O increase significantly with decreasing values of the Ge isotope mass. The results on ^{18}O have been clarified by using an ^{18}O -enriched sample. The broadening of $\nu_3(^{18}\text{O})$ is attributed to some short-range resonance with the three-phonon continuum. It is verified that the Ge and O isotope shifts of this mode are predicted with a good accuracy by a two-parameter semiempirical model. Weak sidebands of $\nu_3(^{16}\text{O})$ have been attributed to transitions involving a change of the value of the rotational quantum number of the O atom rotating about the Ge-Ge axis. An analysis of these transitions allows us to determine the energies of the O rotator in the vibrational ground and excited states for different masses of the Ge atoms. The Ge isotope effect on the rotational energies is found to be much smaller than the one found by phonon spectroscopy on qmi Ge samples. This implies a smaller displacement of the Ge atoms NN of the O atom than estimated previously and phonon resonance measurements on bulk-doped ^{17}O and ^{18}O ^nGe samples could be a valuable test of that point. These results show also the existence at the second order of vibration-rotation transitions without specific selection rules and to our knowledge, such transitions have not been reported before in molecular spectroscopy.

ACKNOWLEDGMENTS

The authors wish to thank Kurt Lassmann for helpful discussions and for sending excerpts from Claus Linsenmaier's Diplomarbeit. They also acknowledge convincing discussions with Hiroshi Yamada-Kaneta. The multireflection sample holder was designed by Denis Côté and Claude Naud. The S sample originated from a crystal grown at

Union Minière Electro-Optic Materials, Olen, Belgium and it was prepared by Nicole Lenain. The low-temperature annealing was performed by Reine-Marie Desfourneaux.

APPENDIX

Average frequencies (cm^{-1}) of the components of the $\nu_3(^{16}\text{O})$ bands in ^{76}Ge at LHeT for the different values of M . The uncertainty is $\pm 0.01 \text{ cm}^{-1}$. The values of frequencies of the $\Delta l=0$ lines used for the attributions of the H and L lines are taken from this list. In this list, different frequencies corresponding to the same value of M have been averaged when necessary. Each line is identified by a value of l and by its common labeling, given in parentheses. The relative intensities (RI's) for each M value are normalized to $M=71$.

The respective intensities at 6 K of components I, II, and III can be appreciated from Fig. 4 for $M=70$ and 75 amu.

0 (I)	± 1 (II)	± 2 (III)	-3 (IV)	M (amu)	RI
863.92	863.85	863.63	863.14	70	0.38
863.40	863.33	863.10	962.62	71	1.00
863.16	863.08	862.86	862.37	71.5	0.29
862.90	862.83	862.60	862.11	72	2.01
862.63	862.56	862.33	861.85	72.5	0.38
862.40	862.33	862.09	861.60	73	2.12
862.14	862.07	861.84	861.36	73.5	0.51
861.90	861.83	861.61	861.12	74	1.57
861.67	861.60	861.37	860.89	74.5	0.11
861.43	861.36	861.13	860.65	75	0.51
860.96	860.89	860.66	860.18	76	0.05

¹J.W. Corbett, R.S. McDonald, and G.D. Watkins, J. Phys. Chem. Solids **25**, 873 (1964).

²B. Pajot and P. Clauws, in *Proceedings of the 18th International Conference on the Physics of Semiconductors*, edited by O. Engström (World Scientific, Singapore, 1987), p. 911.

³E. Artacho, F. Yndurain, B. Pajot, R. Ramirez, C.P. Herrero, L.I. Khirunenko, K. Itoh, and E.E. Haller, Phys. Rev. B **56**, 3820 (1997).

⁴D.R. Bosomworth, W. Hayes, A.R.L. Spray, and G.D. Watkins, Proc. R. Soc. London, Ser. A **317**, 133 (1971).

⁵M. Gienger, M. Glaser, and K. Lassmann, Solid State Commun. **86**, 285 (1993).

⁶H. Yamada-Kaneta, C. Kaneta, and T. Ogawa, Phys. Rev. B **42**, 9650 (1990).

⁷L.I. Khirunenko, V.I. Shakovstov, V.K. Shinkarenko, and F.M. Vorobkalo, Fiz. Tekh. Poluprovodn. **24**, 1051 (1990) [Sov. Phys. Semicond. **24**, 663 (1990)].

⁸A.J. Mayur, M. Dean Sciacca, M.K. Udo, A.K. Ramdas, K. Itoh,

J. Wolk, and E.E. Haller, Phys. Rev. B **49**, 16 293 (1994).

⁹R.E. Whan, Phys. Rev. A **140**, A690 (1965).

¹⁰B. Pajot, E. Artacho, C.A.J. Ammerlaan, and J.M. Spaeth, J. Phys.: Condens. Matter **7**, 7077 (1995).

¹¹W. Kaiser and C.D. Thurmond, J. Appl. Phys. **32**, 115 (1961).

¹²P. Clauws, Mater. Sci. Eng. B **36**, 213 (1996).

¹³P. Clauws and P. Vanmeerbeek, Physica B **273-274**, 557 (1999).

¹⁴B. Pajot, E. Artacho, L.I. Khirunenko, K. Itoh, and E.E. Haller, Mater. Sci. Forum **258-263**, 41 (1997).

¹⁵G. Herzberg, *Molecular Spectra and Molecular Structure II. Infrared and Raman Spectra of Polyatomic Molecules* (Krieger, Malabar, FL, 1991).

¹⁶F. Yndurain, Phys. Rev. Lett. **37**, 1062 (1976).

¹⁷K. Lassmann, C. Linsenmaier, F. Maier, F. Zeller, E.E. Haller, K.M. Itoh, L.I. Khirunenko, B. Pajot, and H. Müssig, Physica B **263-264**, 384 (1999).

¹⁸C. Linsenmaier, Diplomarbeit, Stuttgart, 1998.